

Assessing the Influence of OCT-A Device and Scan Size on Retinal Vascular Metrics

Jessica A. Kraker¹, Bisola S. Omoba¹, Jenna A. Cava², Taly Gilat Schmidt³, Toco Y. Chui^{4,5}, Richard B. Rosen^{4,5}, Judy E. Kim², Joseph Carroll^{2,6}, and Rachel E. Linderman⁶

¹ School of Medicine, Medical College of Wisconsin, Milwaukee, WI, USA

² Department of Ophthalmology and Visual Sciences, Medical College of Wisconsin, Milwaukee, WI, USA

³ Department of Biomedical Engineering, Marquette University and Medical College of Wisconsin, Milwaukee, WI, USA

⁴ Department of Ophthalmology, New York Eye and Ear Infirmary of Mount Sinai, New York, NY, USA

⁵ Icahn School of Medicine at Mount Sinai, New York, NY, USA

⁶ Department of Cell Biology, Neurobiology, and Anatomy, Medical College of Wisconsin, Milwaukee, WI, USA

Correspondence: Rachel Linderman, Department of Cell Biology, Neurobiology, and Anatomy, Medical College of Wisconsin, 925 N 87th Street, Milwaukee, WI 53226-0509, USA.
e-mail: rlinderman@mcw.edu

Received: June 10, 2020

Accepted: September 1, 2020

Published: October 7, 2020

Keywords: optical coherence tomography angiography; foveal avascular zone; imaging; retina; fovea

Citation: Kraker JA, Omoba BS, Cava JA, Gilat Schmidt T, Chui TY, Rosen RB, Kim JE, Carroll J, Linderman RE. Assessing the influence of OCT-A device and scan size on retinal vascular metrics. *Trans Vis Sci Tech.* 2020;9(11):7.
<https://doi.org/10.1167/tvst.9.11.7>

Purpose: The purpose of this study was to investigate the effect of device and scan size on quantitative optical coherence tomography angiography (OCT-A) metrics.

Methods: The 3 × 3 mm scans from Optovue AngioVue and Zeiss AngioPlex systems were included for 18 eyes of 18 subjects without ocular pathology. The foveal avascular zone (FAZ) was segmented manually by two observers, from which estimates of FAZ area (using both the nominal image scale and the axial length corrected image scale) and acircularity were derived. Three scan sizes (3 mm, 6 mm HD, and 8 mm) from the AngioVue system were included for 15 eyes of 15 subjects without ocular pathology. For each subject, larger image sizes were resized to the same resolution as 3 × 3 mm scans, aligned, then cropped to a common area. FAZ area, FAZ acircularity, average and total parafoveal intercapillary area, vessel density, and vessel end points were computed.

Results: Between the devices used here, there were no significant differences in FAZ acircularity ($P = 0.88$) or FAZ area using scaled ($P = 0.11$) or unscaled images ($P = 0.069$). Although there was no significant difference in FAZ area across scan sizes ($P = 0.30$), vessel morphometry metrics were all significantly influenced by scan size.

Conclusions: The scan devices and sizes used here do not affect FAZ area measures derived from manual segmentations. In contrast, vessel morphometry metrics are affected by scan size. As individual differences in axial length induce differences in absolute scan size, extreme care should be taken when interpreting metrics of vessel morphometry, both between and within OCT-A devices.

Translational Relevance: A better characterization of the confounds surrounding OCT-A retinal vasculature metrics can lead to improved application of these metrics as biomarkers for retinal and systemic diseases.

Introduction

Optical coherence tomography angiography (OCT-A) permits noninvasive visualization of retinal capillary perfusion. The widespread availability of this technology has resulted in an enormous growth in the study of retinal vasculature in various systemic and ocular diseases.¹ Of particular interest is the

foveal avascular zone (FAZ) and its surrounding microvasculature, which have been shown to be affected by physiologic sex-associated hormonal changes^{2–4} and diseases, such as diabetic retinopathy,⁵ macular degeneration,⁶ hypertension,⁷ sickle cell disease,⁸ macular telangiectasia,⁹ retinopathy of prematurity,¹⁰ and albinism.¹¹ Central to using OCT-A imagery to diagnose and monitor conditions like these is the ability to extract quantitative metrics describing

the retinal vasculature. However, there are a number of nonbiological factors that affect retinal vasculature metrics, including scan size, processing algorithm, slab definition, image quality, and motion artifacts. These factors can all vary between or even *within* devices, potentially limiting the translational utility of OCT-A.

Following the model of studies examining structural OCT measurements, such as retinal thickness,^{12,13} there have been dozens of studies looking at the impact of device model/manufacture on a number of OCT-A vasculature metrics. These studies have examined clinical performance,^{14,15} FAZ area,^{16–23} and vessel density.^{18–20,24–26} With only a couple of exceptions, the general consensus of these studies is that agreement of quantitative metrics between devices is poor. With respect to FAZ area, one possible explanation may be that very few studies consider individual differences in lateral magnification of the retinal image, which are largely due to variations in axial length.²⁷ As the assumed axial length of the various OCT-A devices differs—and in some cases is not even known to users—these discrepancies could underlie at least some of the reported differences in FAZ area between devices.

Studies on the effect of OCT-A scan size are considerably more limited. Although many support a greater “clinical utility” of larger scan sizes^{15,28} or have examined particular disease states, such as glaucoma,^{29,30} age-related macular degeneration,³¹ and choroidal neovascularization,³² relatively few have examined the impact of scan size on the quantitative vascular metrics of interest here. Moreover, there are some conflicting results as to whether vascular metrics are interchangeable between different scan sizes. For example, Dong et al. concluded that FAZ area is interchangeable between 3×3 mm and 6×6 mm scan sizes using the AngioVue, but found a significant reduction in vessel density in 6×6 mm scans.³³ Similarly, Rabiolo et al. showed that FAZ area was interchangeable across 3×3 mm, 6×6 mm, and 12×12 mm scan sizes using the AngioPlex, but that vessel density was highly dependent on scan size.³⁴ In contrast, Chen et al. reported a $\sim 10\%$ difference in FAZ area between 3×3 mm and 6×6 mm scan sizes (0.234 mm^2 and 0.259 mm^2 , respectively)³⁵ but nonsignificant vessel density differences when using the AngioVue.³⁵ In studies comparing scan size, the issue of image magnification is less critical, as we are only interested in *relative* differences between scan dimensions from the same device. However, it is known that averaging multiple en face OCT-A images can significantly improve signal-to-noise ratio;^{4,36–39} thus the use of averaged images could allow a more direct evaluation of the impact of scan size on quantitative vascular metrics. This is important,

as multiple studies have found that the reliability and/or repeatability of various vascular metrics tends to be worse for larger scan sizes.^{35,40}

In summary, the existing studies to date examining the reproducibility of OCT-A metrics across scan device and size are limited by the fact that: (1) they only examine the quantitative metrics of FAZ area and vessel density; (2) they use the assumed axial length inherent to the imaging device; and (3) they use unaveraged images, which have a limited ability to derive information from larger scan sizes. Here, we attempted to rectify these methodological shortcomings by isolating the effect of device model and scan size choice on quantitative OCT-A metrics. We performed two parallel but complementary experiments varying *either* the scan device (Zeiss AngioPlex and Optovue AngioVue) or the scan size (3×3 mm, 6×6 mm HD, and 8×8 mm) used to acquire OCT-A images. If OCT-A metrics were truly reproducible across these methodologic variables, those interpreting these metrics could know with absolute certainty that differences in observed metrics reflect actual differences in retinal vasculature.

Methods

Subject Selection

This study was approved by the Institutional Review Board of the Medical College of Wisconsin (PRO23999) and followed the tenets of the Declaration of Helsinki. Written informed consent was obtained from all subjects after explanation of the procedures and potential risks of the study. Exclusion criteria included any subjects under the age of 5 years and subjects with self-reported ocular or systemic vascular disease. Axial length measurements were acquired for all individuals using an IOLMaster (Carl Zeiss Meditec, Dublin, CA).

Image Acquisition and Processing

Experiment 1 (Device Model Selection)

The right eyes of 20 subjects were imaged on the same day using both the AngioVue (Optovue, Inc., Fremont, CA) and the AngioPlex (Carl Zeiss Meditec) systems. The order in which scans were taken using each device was randomized. For the AngioVue system, two volumes, each consisting of 304 B-scans at 304 A-scans / B-scan were acquired centered on the fovea. The two volumes were co-registered (AngioVue software version: 2017.1.0.151) to create one volume scan at a nominal scan size of 3×3 mm and a

custom retinal slab (3 μm above the inner limiting membrane [ILM] to 16 μm below the inner plexiform layer [IPL]) was used for further analysis. For the AngioPlex system, a single nominal 3 \times 3 mm volume scan (245 B-scans at 245 A-scans / B-scan acquired in the fast X direction) was acquired centered on the fovea. The superficial slab (ILM to IPL) with an image size of 1024 \times 1024 pixels was extracted for analysis. Bicubic interpolation was used to resample the AngioVue scans to the same nominal image scale ($\mu\text{m}/\text{pixel}$) as the AngioPlex scans using Adobe Photoshop prior to further analysis (Adobe Systems Inc., Mountain View, CA).

Experiment 2 (Scan Size Selection)

The right eyes of 19 subjects were imaged using the AngioVue system (Optovue, Inc.). Eleven of these subjects also participated in the device experiment described above. Ten volume scans were acquired for 3 nominal scan sizes (3 \times 3 mm, 6 \times 6 mm HD, and 8 \times 8 mm) for a total of 30 scans per eye. The order in which each set of 10 scans per nominal scan size was acquired was randomized. The 6 \times 6 mm HD scans consisted of 400 B-scans at 400 A-scans / B-scan, whereas both the 3 \times 3 mm and the 8 \times 8 mm scans consisted of 304 B-scans at 304 A-scans / B-scan. For each volume scan, a custom slab (3 μm above the ILM to 16 μm below the IPL) was extracted for analysis.

For all angiograms, image quality was assessed using a Sobel filter to measure the mean gradient magnitude as previously described.³⁶ For each scan size per subject, the five frames with the highest mean gradient magnitude were registered and averaged using Stack-Reg plugin⁴¹ on ImageJ⁴² to create a single averaged image, for a total of 45 final images. Each subject's larger 6 \times 6 mm HD and 8 \times 8 mm scans were resampled to the same scale as their 3 \times 3 mm scan using bicubic interpolation in Adobe Photoshop (Adobe Systems Inc., Mountain View, CA) prior to further analysis.

Quantitative Retinal Vasculature Analysis

Foveal Avascular Zone Analysis (Experiments 1 and 2)

Prior to analysis of the FAZ, it was necessary to remove subjects having "fragmented" FAZs (also known as macular-foveal capillaries),⁴³ as the absence of a single well-defined FAZ would confound our analyses. A 3 \times 3 mm image from each of the 28 participants was analyzed using a previously described custom MATLAB script,⁴³ generating measurements of each intercapillary area within 1.3 mm of the center of the foveal pit for each subject. For the 9 subjects that only participated in the device comparison study

(experiment 1), a single unaveraged 3 \times 3 mm image was used, whereas an averaged 3 \times 3 mm image was used for the other 19 subjects that participated in the size comparison study (experiment 2). For each image, the ratio between the largest intercapillary area and each intercapillary area was calculated. A subject was classified as having a fragmented FAZ if they had two or more intercapillary areas to FAZ ratios of 0.3 or greater, indicating vessel(s) bisecting an otherwise avascular area.⁴³ In total, two subjects were removed from both experiments and two additional subjects were removed from the scan size study (experiment 2). This resulted in 18 subjects remaining for experiment 1 and 15 subjects remaining for experiment 2.

For the remaining images, the FAZ was manually segmented by two observers (J.A.K. and R.E.L.) masked to the other's segmentation using ImageJ's multipoint tool.⁴² The segmentation coordinates were entered into a custom MATLAB script based on previous work in our laboratory.^{44,45} The area of the FAZ (in pixels) was computed using the `poly2area` function. The perimeter of the FAZ (in pixels) was calculated by summing the distance between each pair of neighboring segmentation coordinates. The area and perimeter were converted from pixels to absolute retinal measurements (in millimeters) by multiplying by the real scale of that image.³⁶ The real scale of each image was calculated as follows:

$$\text{real image scale (mm/px)} = \text{nominal image scale (mm/px)} \\ \times \frac{\text{measured axial length (mm)}}{\text{assumed model eye length (mm)}}$$

Acircularity is a unitless metric generated from estimates of the FAZ area and FAZ perimeter, and was calculated as follows:

$$\text{Acircularity} = \left(\frac{\text{FAZ Perimeter}}{2 * \pi * \sqrt{\frac{\text{FAZ Area}}{\pi}}} \right)$$

Additionally, for the image device experiment only, each segmentation was re-run through MATLAB *without* correcting for individual axial length and instead using the assumed model eye axial length (23.95 mm and 24.46 mm for the AngioVue and AngioPlex, respectively) to generate unscaled FAZ area measurements for each device.

Vascular Morphometry Analysis (Experiment 2)

Vessel density and parafoveal intercapillary area (PICA) were derived for each image using a custom MATLAB script.⁴⁶ Vessel density was calculated across the whole image, including the FAZ. For the PICA metrics, the largest intercapillary area (corresponding

Table 1. Interobserver Agreement Analysis for FAZ Area

	Unaveraged 3 × 3 mm AngioPlex	Unaveraged 3 × 3 mm AngioVue	Averaged 3 × 3 mm AngioVue	Averaged 6 × 6 mm HD AngioVue	Averaged 8 × 8 mm AngioVue
Reproducibility^a	0.006 mm ²	0.007 mm ²	0.011 mm ²	0.018 mm ²	0.047 mm ²
Measurement Error^b	0.004 mm ²	0.005 mm ²	0.008 mm ²	0.012 mm ²	0.033 mm ²
ICC (95% CI)	0.9993(0.9986–0.9999)	0.9991(0.9983–1.000)	0.9976(0.9951–1.000)	0.9930(0.9858–1.000)	0.9597(0.9190–1.000)

^aDifferences between measurements from two observers of the same subject would be expected to be less than this value for 95% of pairs of measurements.⁴⁹

^bThe difference between a subject's measurement and the true value would be expected to be less than this value for 95% of observations.⁴⁹

to the FAZ) was manually subtracted from the raw data before average PICA and total (summed) PICA were calculated for the remainder of the image. Images were binarized and skeletonized in ImageJ, and then run through AnalyzeSkeleton 2D/3D⁴⁷ in FIJI⁴⁸ to generate the total number of vessel endpoints in the entire image.

Statistical Analysis

Experiment 1 (Device Model Selection)

Reproducibility, measurement error (as defined by Bland & Altman [1996]⁴⁹), and intraclass correlation coefficient (ICC; R Foundation for Statistical Computing, Vienna, Austria) were calculated to assess the interobserver agreement for the 3 × 3 mm scans from each device. To test for differences between devices, FAZ area and acircularity were assessed both with and without individual axial length correction. For each comparison, either a paired *t*-test or a Wilcoxon matched-pairs signed rank test were performed (Prism version 8.4.1, GraphPad Software, La Jolla, CA). The decision for which test to use was based on an analysis of normality ($P < 0.05$) of the difference between the two devices using the Shapiro-Wilk normality test (Prism).

Experiment 2 (Scan Size Selection)

Reproducibility, measurement error (as defined by Bland & Altman [1996]⁴⁹), and ICC (R Foundation for Statistical Computing) were calculated to assess the interobserver agreement for each scan size using the AngioVue device. To test for differences between scan sizes, either a repeated measures 1-way ANOVA or a Friedman test was performed (Prism) for each retinal vasculature metric. The decision for which test to use was based on an analysis of normality ($P < 0.05$) for each of the three scan sizes using the Shapiro-Wilk normality test (Prism). Due to the multiple statistical tests run, a *P* value of 0.0083 or smaller was considered significant. If significant differences were

found, a Tukey or Dunn's post hoc test was performed with significance again set at < 0.0083 .

Results

Subject Demographics

For experiment 1 (device model selection), we included 18 subjects in the final analysis (3 males and 15 females) with an average age of 31.33 years (range = 20–63 years), an average axial length of 24.05 mm, and self-identifying as white (17) and Asian (1). For experiment 2 (scan size selection), we included 15 subjects in the final analysis (3 males and 12 females) with an average age of 29.93 years (range = 23–50 years), an average axial length of 24.24 mm, and self-identifying as white (10), Asian (3), black (1), and Hispanic (1).

Interobserver Reproducibility

There was excellent agreement between the two masked observers for all scan types, although the agreement decreased slightly for the larger scan sizes (see Table 1). That said, the largest interobserver measurement error for the averaged 8 × 8 mm AngioVue scan was only 0.032 mm² (about 10% of the mean FAZ area). All further analysis was performed on the observers' averaged values for FAZ metrics (FAZ area and FAZ acircularity). Because the remaining metrics (PICA, vessel density, and vessel endpoints) are extracted automatically without requiring segmentation, no reproducibility examination was performed for these metrics.

Foveal Avascular Zone Metrics

Experiment 1 (Scan Device Selection)

As shown in Figure 1, there were no significant differences between devices (AngioPlex–AngioVue)

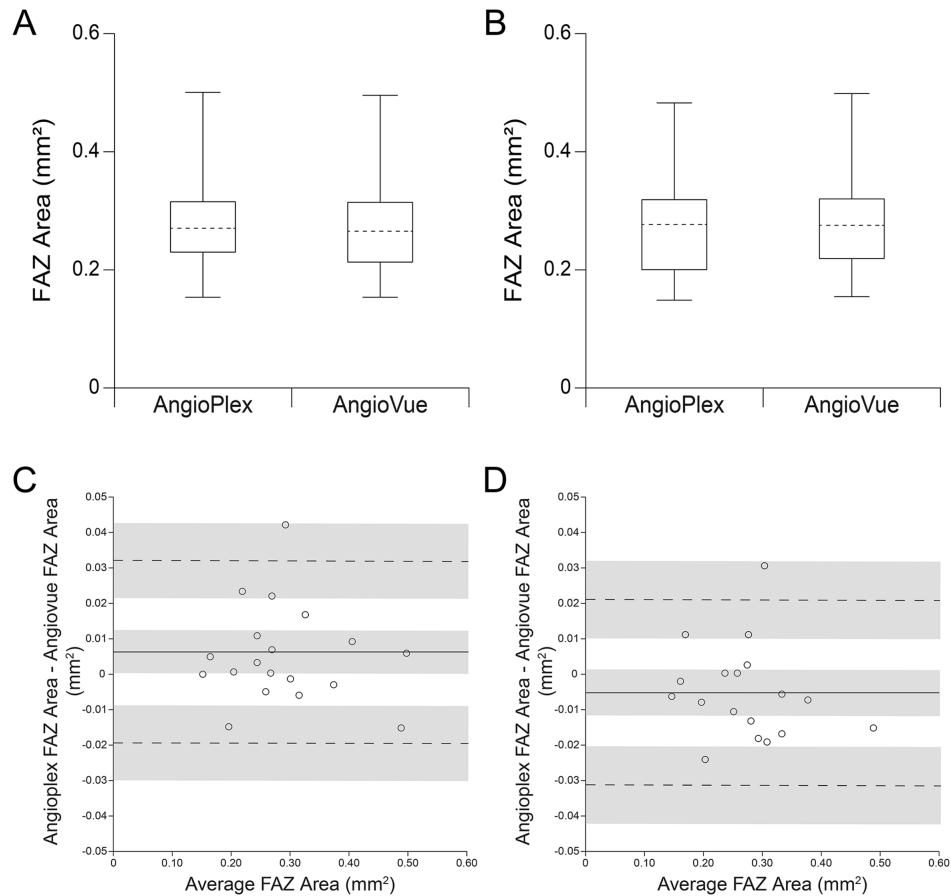


Figure 1. Comparison of the FAZ area with unscaled and scaled data. **(A)** Unscaled FAZ area measurements (average of 2 observers) of 18 right eyes taken using unaveraged 3×3 mm images for each scan device (AngioVue, AngioPlex). **(B)** Scaled FAZ area measurements of the 18 right eyes (*dashed lines*: median; box limits: 25th to 75th percentiles; whiskers: minimum and maximum). There were no significant differences in FAZ area (AngioPlex–AngioVue) between devices using either unscaled (paired *t*-test, average difference: 0.006 mm^2 , $P = 0.069$) or scaled measurements (paired *t*-test, average difference: -0.005 mm^2 , $P = 0.11$). Scaling resulted in decreased average FAZ area (mean \pm SD) when using the AngioPlex (unscaled area: $0.281 \pm 0.087 \text{ mm}^2$; unscaled range: $0.152\text{--}0.501 \text{ mm}^2$; scaled area: $0.271 \pm 0.083 \text{ mm}^2$; scaled range: $0.147\text{--}0.483 \text{ mm}^2$) but increased average FAZ area (mean \pm SD) when using the AngioVue (unscaled area: $0.275 \pm 0.086 \text{ mm}^2$; unscaled range: $0.152\text{--}0.496 \text{ mm}^2$; scaled area: $0.276 \pm 0.085 \text{ mm}^2$; scaled range: $0.153\text{--}0.499 \text{ mm}^2$). **(C)** Bland-Altman plot showing interdevice agreement for unscaled average FAZ area. **(D)** Bland-Altman plot showing interdevice agreement for scaled average FAZ area. *Solid lines* represent the mean difference (bias) between the devices, *dotted lines* represent limits of agreement (LOA), gray shading represents the 95% confidence intervals for the bias and LOAs for each device.

using either unscaled (paired *t*-test, average difference: 0.006 mm^2 , $P = 0.069$) or scaled (paired *t*-test, average difference: -0.005 mm^2 , $P = 0.11$) measurements of FAZ area. Scaling resulted in decreased average FAZ area (mean \pm SD) when using the AngioPlex (unscaled: $0.281 \pm 0.087 \text{ mm}^2$; and scaled: $0.271 \pm 0.083 \text{ mm}^2$) but increased FAZ area when using the AngioVue (unscaled: $0.275 \pm 0.086 \text{ mm}^2$; and scaled: $0.276 \pm 0.085 \text{ mm}^2$). FAZ acircularity does not require correction for ocular magnification,⁵⁰ so no scaling comparison was necessary. Although there were some subjects with visible distortion in the FAZ contour between devices (Supplementary Video S1), there was no significant difference in FAZ acircularity between devices

(mean \pm SD: AngioVue = 1.19 ± 0.09 ; AngioPlex = 1.21 ± 0.12 ; $P = 0.88$, Wilcoxon signed-rank test). In other subjects, minimal inter-device distortion was present (Supplementary Video S2).

Experiment 2 (Scan Size Selection)

FAZ area did not significantly differ across the three scan sizes (Fig. 2; Table 2; Supplementary Fig. S1). Representative OCT-A images from subjects with the best, median, and worst agreement in FAZ area (based on the variance across the three scan sizes) are shown in Figure 3. FAZ acircularity decreased as the scan size increased, meaning that the FAZ shape

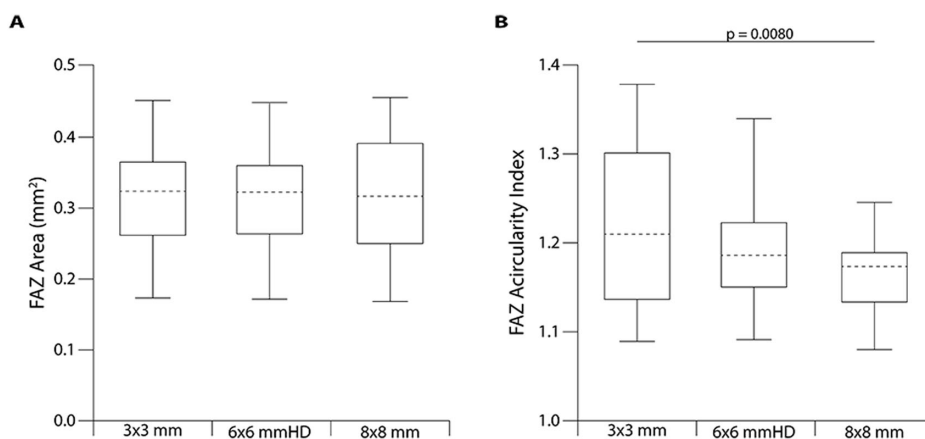


Figure 2. Box-whisker plots of (A) average FAZ area and (B) FAZ acircularity of 15 right eyes taken using the AngioVue device at three scan sizes (3×3 mm, 6×6 mm HD, and 8×8 mm) using averaged frames. The *horizontal dashed lines* represent the median, the *boxes* represent the upper and lower quartiles, and the *tick marks* represent the minimum and maximum values.

Table 2. Average Retinal Vasculature Metrics (Mean \pm SD) of 3×3 mm, 6×6 mm HD, and 8×8 mm AngioVue Scans^a

	3×3 mm	6×6 mm HD	8×8 mm	ANOVA <i>P</i> Value	3 vs. 6 <i>P</i> Value	3 vs. 8 <i>P</i> Value	6 vs. 8 <i>P</i> Value
FAZ area (mm²)^b	0.316 \pm 0.08	0.313 \pm 0.08	0.321 \pm 0.08	0.2963	NA	NA	NA
FAZ acircularity Index^b	1.23 \pm 0.09	1.19 \pm 0.07	1.17 \pm 0.05	0.0018	0.0437	0.0080	0.1315
Average PICA (μm^2)^b	2003 \pm 248	2612 \pm 415	7820 \pm 2127	<0.0001	<0.0001	<0.0001	<0.0001
Total PICA (mm²)^b	3.78 \pm 0.44	3.86 \pm 0.49	4.55 \pm 0.56	<0.0001	0.0017	<0.0001	<0.0001
Vessel density (%)^c	49.0 \pm 1.15	49.3 \pm 0.722	42.8 \pm 1.53	<0.0001	>0.9999	0.0002	<0.0001
Total end points (No.)^b	1872 \pm 276	1535 \pm 96	484 \pm 119	<0.0001	0.0005	<0.0001	<0.0001

NA, not applicable as *P* value from ANOVA was not statistically significant.

^aAll analysis performed on images scaled using the subject's axial length.

^bEvaluated using 1-way repeated measures ANOVA and a Tukey post hoc test.

^cEvaluated using a Friedman nonparametric test and a Dunn's post hoc test.

became more circular as the scan area became larger (see Table 2).

As shown in Figure 4, Table 2, and Supplementary Figure S2 there were significant differences between at least two of the three scan sizes for each retinal vasculature metric examined (i.e. PICA, vessel density, and vessel endpoints). There was a significant decrease in vessel density measured using 8×8 mm scans as compared to either 3×3 mm scans ($P = 0.0002$) or 6×6 mm HD scans ($P < 0.0001$), although there was no difference in vessel density between 3×3 mm and 6×6 mm HD scans (see Table 2). As the size of the scan increased, average PICA and total PICA also increased (see Table 2). The inverse was found with vessel endpoints; as scan size increased, the total number of endpoints decreased (see Table 2).

Discussion

Here, we show that the choice of device (AngioVue or AngioPlex) does not have a significant effect on FAZ metrics in either unscaled or correctly scaled images when using manual segmentation. We also evaluated the effect of scan size on retinal vasculature and found that while scan size does not significantly impact measurements of FAZ area, it does affect FAZ acircularity and other measures of vessel morphology, such as vessel density, PICA, and number of vessel endpoints. This supports the idea that these metrics, which are intuitively more dependent on scan resolution, are not interchangeable across different scan sizes.

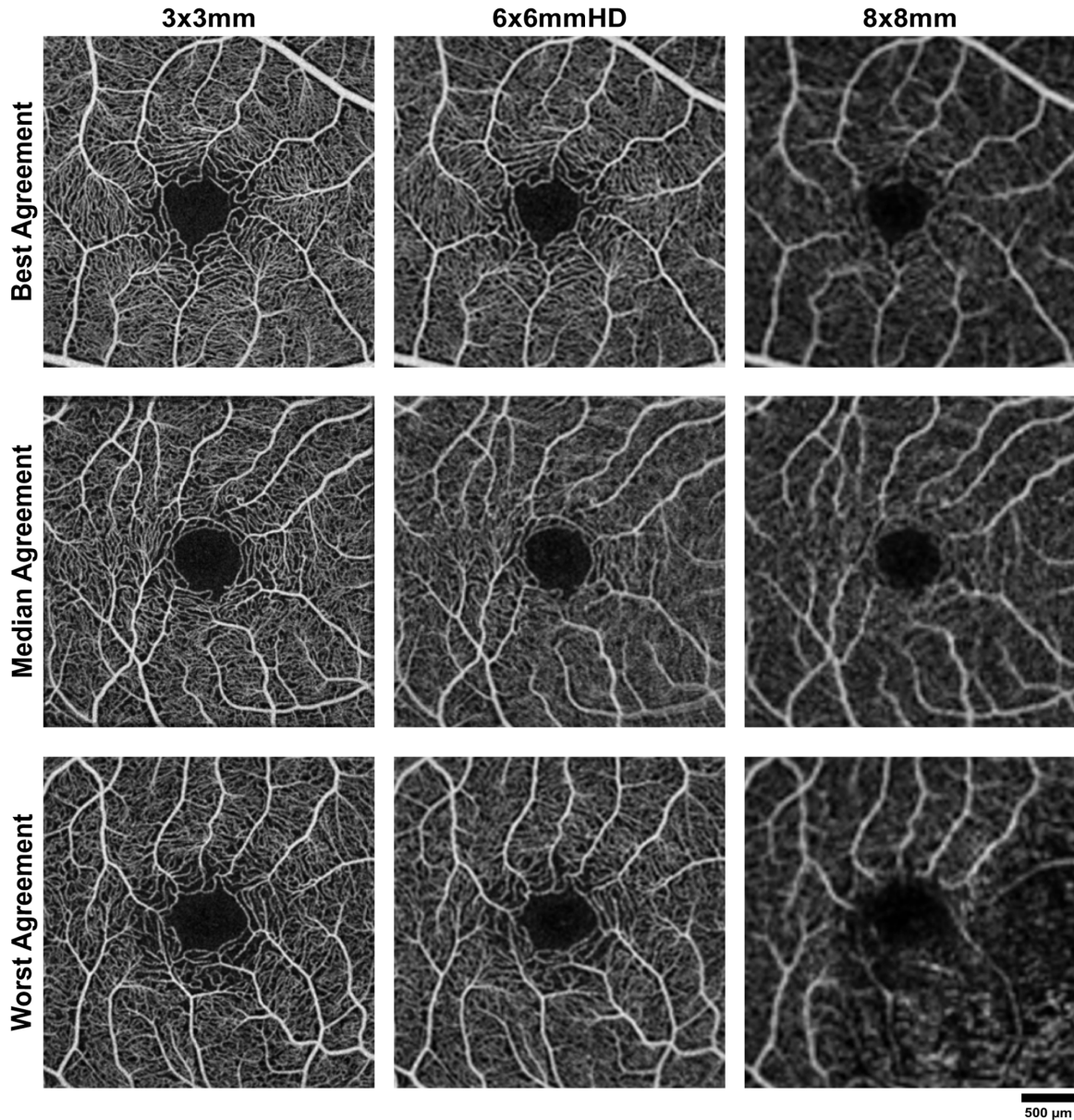


Figure 3. Agreement in FAZ area across scan size. Averaged, cropped, and scaled images from three subjects with the best ($\sigma^2 = 5.63E-07$), median ($\sigma^2 = 1.52E-05$), and worst ($\sigma^2 = 0.002395$) agreement in FAZ area across all scan sizes (3×3 mm, 6×6 mm HD, and 8×8 mm) acquired using the AngioVue device. Scale bar = $500 \mu\text{m}$.

Previous studies have shown that errors in image scale^{27,51} and differing segmentation methods^{19,38} can affect measurements of FAZ area.^{15,16,18,19,22,23,52} Strengths of our study are that: (1) we used manual segmentation of the FAZ contour and (2) we used the subject's axial length and knowledge of the assumed axial for each device to derive the image scale for each OCT-A image. This approach allowed us to isolate the impact of the OCT-A device on FAZ metrics. Interestingly, we observed no difference in FAZ area between devices regardless of whether we used scaled or unscaled images. However, we did observe

a small effect of scaling within each device; the use of correct scaling resulted in an average *decrease* in FAZ area of 0.01 mm^2 when using the AngioPlex and an average *increase* in FAZ area of 0.001 mm^2 when using the AngioVue. This small and opposing effect of scaling is due to the average axial length of our cohort being slightly greater than the assumed axial length of the AngioVue device but slightly less than the assumed axial length of the AngioPlex device. Taken together, our findings suggest that previously reported differences in FAZ area between different OCT-A devices^{15,16,18,19,22,23,52} are most likely due to

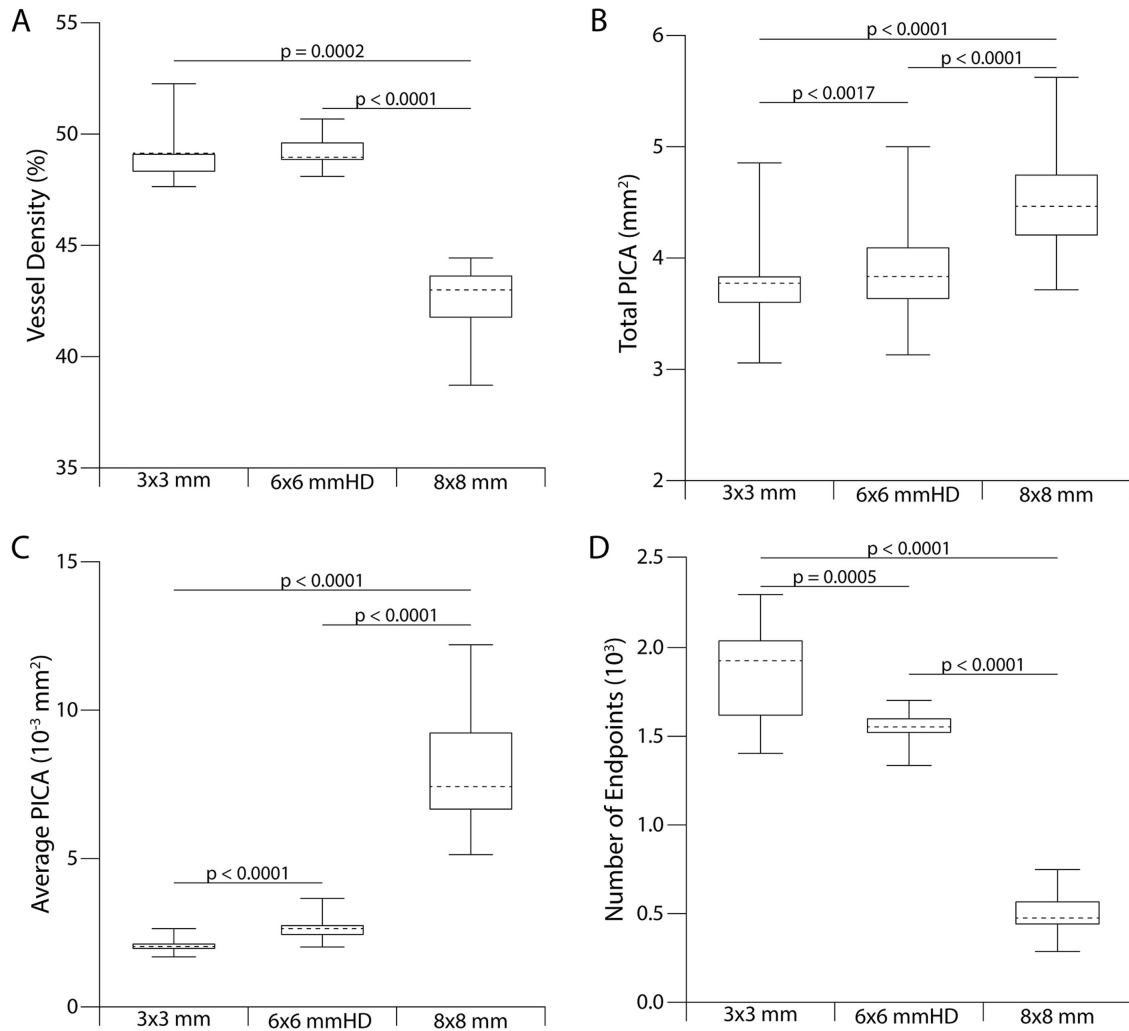


Figure 4. Box-whisker plots of (A) vessel density, (B) total parafoveal intercapillary area (PICA), (C) average PICA, and (D) total number of vessel endpoints of 15 right eyes taken using the AngioVue device at three scan sizes (3 × 3 mm, 6 × 6 mm HD, and 8 × 8 mm) using averaged frames. The horizontal dashes represent the median, the boxes represent the upper and lower quartiles, and the tick marks represent the minimum and maximum values.

different postprocessing methods inherent to the devices as opposed to fundamental differences in the images themselves. Additionally, it is possible that the axial length characteristics of the subjects in earlier studies differed relative to the device(s) used, which would affect the reported relative differences in FAZ area between devices.

OCT-A scan size does not seem to affect superficial FAZ area metrics, supporting some previous studies^{33,34} and refuting others.³⁵ In contrast, scan size was found to significantly affect all metrics of vessel morphometry (FAZ acircularity, average and total PICA, vessel density, and vessel endpoints). To understand the basis for this finding, one needs to consider not just the scan dimensions but also the number of A-scans and B-scans within the volume.

The nominal scan sizes of 3 × 3 mm, 6 × 6 mm HD, and 8 × 8 mm equate to image resolutions of 9.9 μm/px, 15 μm/px, and 26.3 μm/px, respectively. The sensitivity of metrics of vessel morphometry to scan size would suggest that the axial length may not only affect measures of FAZ area by altering the scale of the image,^{27,51} but also may affect the integrity of metrics of vessel morphometry by altering the effective image resolution across subjects. Indeed, factoring in variation in axial length in our cohort, we find that the effective image resolution ranges from 9.2 to 11.1 μm/px for the 3 × 3 mm scans, 14.0 to 16.8 μm/px for the 6 × 6 mm HD scans, and 24.5 to 29.7 μm/px for the 8 × 8 mm scans. It is important to note that the range of axial lengths in our subject population was relatively small, and so the differences in effective image

resolution could be even greater in different populations. This has important implications for considering any of these metrics as possible biomarkers, as the metrics would have different sensitivities across different subjects according to their axial length. This cannot be mitigated with postprocessing, as parameters of the scans themselves (such as sampling density discussed here) would need to be adjusted for axial length *prior to* acquisition to ensure uniform image resolution across patients in a given study. Although such efforts may not be practical in a busy clinical setting, it would be imperative for studies aiming to characterize disease progression or evaluate therapeutic efficacy on a patient by patient basis.

There are important limitations to our study. First, our results are only applicable to the devices (AngioVue and AngioPlex), scan sizes (3×3 mm, 6×6 mm HD, and 8×8 mm), and capillary plexus (superficial) examined here. Given the wide variability in devices and scan settings, it is not possible to extrapolate our findings to other combinations of scan device, scan size, or deeper capillary plexuses. Second, our subject population skewed female, young, white, emmetropic, and without known ocular pathology. We cannot rule out that a more diverse population may reveal device-specific differences in FAZ area within subgroups, such as sex, age, ethnicity, refractive error, or ocular pathology. A third limitation is our small sample size. For the device comparison, we were powered to detect a difference in FAZ area of 0.04 mm^2 assuming an alpha of 0.05 and a power of 0.8. Although we did not observe a significant difference in FAZ area between devices, it could be that we were underpowered to detect a small but significant difference. We can, however, say that *if* there is a significant difference between devices, it does not exceed 0.04 mm^2 .

As evidenced in our experiments, a tradeoff exists between image resolution and field-of-view; small scan sizes provide the highest resolution images of capillaries at the expense of retina-wide information.⁵³ This tradeoff can be compensated for via montaging multiple smaller high-quality images or by utilizing frame averaging with larger images to improve the signal-to-noise ratio.^{4,36–39} Whereas montaging and averaging are feasible in a research setting, they have not yet reached widespread use – this can be remedied with software advances. Future studies may be able to identify the optimal scan size that gives reliable measures of vessel morphometry without sacrificing the scan area. Of course, “chair time” must also be considered in such evaluations, as longer scan acquisition increases the likelihood that there will be artifacts, such as blinks, distortion from eye motion, and reduced image quality due to tear film degradation.

Nevertheless, there is a need for further prospective studies that systematically alter sampling density within the same subject to empirically determine the analytical limits of OCT-A.

Acknowledgments

The authors thank Erin Curran, Vesper Williams, and Erica Woertz for help recruiting and imaging subjects, Heather Heitkotter for help editing the manuscript, and Sergey Tarima for his help with our statistical analysis.

Supported in part by the National Eye Institute and the National Center for Advancing Translational Sciences of the National Institute of Health (NIH) under award numbers T32EY014537, R01EY024969, UL1TR001436, and R01EY027301. This investigation was conducted in a facility constructed with support from the Research Improvement Program, Grant Number C06RR016511, from the National Center for Research Resources, NIH. The content is solely the responsibility of the authors and does not necessarily represent the official views of the NIH. Additional support given from the Gene and Ruth Posner Foundation and the Vision for Tomorrow Foundation.

Disclosure: **J.A. Kraker**, None; **B.S. Omoba**, None; **J.A. Cava**, None; **T. Gilat Schmidt**, GE Healthcare (F); **T.Y. Chui**, None; **R.B. Rosen**, Advanced Cellular Technologies (C), Carl Zeiss Meditech (C), Clarity, NanoRetina (C), OD-OS (C), Optovue (C), and Regeneron (C), Opticology (I); **J.E. Kim**, Notal Vision (F), Optos (F), Adverum (C), Allergan (C), Alimera Science (C), Clearside (C), Gemini (C), Genentech (C), Kodiak (C), Notal Vision (C), and Novartis (C); **J. Carroll**, Optovue (F), AGTC (F), MeiraGTx (F), MeiraGTx (C), and Translational Imaging Innovations (I); **R.E. Linderman**, Optovue (C)

References

1. Fujimoto J, Swanson E. The development, commercialization, and impact of optical coherence tomography. *Invest Ophthalmol Vis Sci*. 2016;57:1–13.
2. Gómez-Ulla F, Cutrin P, Santos P, et al. Age and gender influence on foveal avascular zone in healthy eyes. *Exp Eye Res*. 2019;189:107856.
3. Shahlaee A, Pefkianaki M, Hsu J, Ho AC. Measurement of foveal avascular zone dimensions and

- its reliability in healthy eyes using optical coherence tomography angiography. *Am J Ophthalmol.* 2016;161:50–55.
4. Uji A, Balasubramanian S, Lei J, Baghdasaryan E, Al-Sheikh M, Sadda SR. Choriocapillaris imaging using multiple en face optical coherence tomography angiography image averaging. *JAMA Ophthalmol.* 2017;135:1197–1204.
 5. Tam J, Dhamdhare KP, Tiruveedhula P, et al. Subclinical capillary changes in non-proliferative diabetic retinopathy. *Optom Vis Sci.* 2012;89:E692–E703.
 6. Lindner M, Fang PP, Steinberg JS, et al. OCT angiography-based detection and quantification of the neovascular network in exudative AMD. *Invest Ophthalmol Vis Sci.* 2016;57:6342–6348.
 7. Lee WH, Park JH, Won Y, et al. Retinal microvascular change in hypertension as measured by optical coherence tomography angiography. *Sci Rep.* 2019;9:156.
 8. Sanders RJ, Brown GC, Rosenstein RB, Magargal L. Foveal avascular zone diameter and sickle cell disease. *Arch Ophthalmol.* 1991;109:812–815.
 9. Dogan B, Erol MK, Akidan M, Suren E, Akar Y. Retinal vascular density evaluated by optical coherence tomography angiography in macular telangiectasia type 2. *Int Ophthalmol.* 2019;39:2245–2256.
 10. Bowl W, Bowl M, Schweinfurth S, et al. OCT angiography in young children with a history of retinopathy of prematurity. *Ophthalmol Retina.* 2018;2:972–978.
 11. Wilk MA, McAllister JT, Cooper RF, et al. Relationship between foveal cone specialization and pit morphology in albinism. *Invest Ophthalmol Vis Sci.* 2014;55:4186–4198.
 12. Pierro L, Giatsidis SM, Mantovani E, Gagliardi M. Macular thickness interoperator and intraoperator reproducibility in healthy eyes using 7 optical coherence tomography instruments. *Am J Ophthalmol.* 2010;150:199–204.
 13. Wolf-Schnurrbusch UE, Ceklic L, Brinkmann CK, et al. Macular thickness measurements in healthy eyes using six different optical coherence tomography instruments. *Invest Ophthalmol Vis Sci.* 2009;50:3432–3437.
 14. Ghassemi F, Mirshahi R, Bazvand F, Fadakar K, Faghihi H, Sabour S. The quantitative measurements of foveal avascular zone using optical coherence tomography angiography in normal volunteers. *J Curr Ophthalmol.* 2017;29:293–299.
 15. Li XX, Wu W, Zhou H, et al. A quantitative comparison of five optical coherence tomography angiography systems in clinical performance. *Int J Ophthalmol.* 2018;11:1784–1795.
 16. Trachsler S, Baston AE, Menke M. Intra- and interdevice deviation of optical coherence tomography angiography. *Klin Monbl Augenheilkd.* 2019;236:551–554.
 17. Dave PA, Dansingani KK, Jabeen A, et al. Comparative evaluation of foveal avascular zone on two optical coherence tomography angiography devices. *Optom Vis Sci.* 2018;95:602–607.
 18. Corvi F, Pellegrini M, Erba S, Cozzi M, Staurenghi G, Giani A. Reproducibility of vessel density, fractal dimension, and foveal avascular zone using 7 different optical coherence tomography angiography devices. *Am J Ophthalmol.* 2018;186:25–31.
 19. Magrath GN, Say EAT, Sioufi K, Ferenczy S, Samara WA, Shields CL. Variability in foveal avascular zone and capillary density using optical coherence tomography angiography machines in healthy eyes. *Retina.* 2017;37:2102–2111.
 20. Lu Y, Wang JC, Zeng R, et al. Quantitative comparison of microvascular metrics on three optical coherence tomography angiography devices in chorioretinal disease. *Clin Ophthalmol.* 2019;13:2063–2069.
 21. Chung CS, Nesper PL, Park JJ, Fawzi AA. Comparison of Zeiss cirrus and Optovue RTVue OCT angiography systems: a quantitative and qualitative approach examining the three capillary networks in diabetic retinopathy. *Ophthalmic Surg Lasers Imaging Retina.* 2018;49:198–205.
 22. Mihailovic N, Brand C, Lahme L, et al. Repeatability, reproducibility and agreement of foveal avascular zone measurements using three different optical coherence tomography angiography devices. *PLoS One.* 2018;13(10):e0206045.
 23. Pilotto E, Frizziero L, Crepaldi A, et al. Repeatability and reproducibility of foveal avascular zone area measurement on normal eyes by different optical coherence tomography angiography instruments. *Ophthalmic Res.* 2018;59(4):206–211.
 24. Yang J, Yuan M, Wang E, Chen Y. Comparison of the repeatability of macular vascular density measurements using four optical coherence tomography angiography systems. *J Ophthalmol.* 2019;2019:4372580.
 25. Munk MR, Giannakaki-Zimmermann H, Berger L, et al. OCT-angiography: a qualitative and quantitative comparison of 4 OCT-A devices. *PLoS One.* 2017;12(5):E0177059.
 26. Lei J, Pei C, Wen C, Abdelfattah NS. Repeatability and reproducibility of quantification of superficial peri-papillary capillaries by four different optical

- coherence tomography angiography devices. *Sci Rep*. 2018;8:17866.
27. Llanas S, Linderman RE, Chen FK, Carroll J. Assessing the use of incorrectly scaled optical coherence tomography angiography images in peer-reviewed studies: a systematic review. *JAMA Ophthalmol*. 2020;138:86–94.
 28. Ho J, Dans K, You Q, Nudleman ED, Freeman WR. Comparison of 3 mm x 3 mm versus 6 mm x 6 mm optical coherence tomography angiography scan sizes in the evaluation of non-proliferative diabetic retinopathy. *Retina*. 2019;39:259–264.
 29. Chang R, Chu Z, Burkemper B, et al. Effect of scan size on glaucoma diagnostic performance using OCT angiography en face images of the radial peripapillary capillaries. *J Glaucoma*. 2019;28:465–472.
 30. Kwon J, Shin JW, Lee J, Kook MS. Choroidal microvasculature dropout is associated with parafoveal visual field defects in glaucoma. *Am J Ophthalmol*. 2018;188:141–154.
 31. Chu Z, Gregori G, Rosenfeld PJ, Wang RK. Quantification of choriocapillaris with optical coherence tomography angiography: a comparison study. *Am J Ophthalmol*. 2019;208:111–123.
 32. Miller AR, Roisman L, Zhang Q, et al. Comparison between spectral-domain and swept-source optical coherence tomography angiographic imaging of choroidal neovascularization. *Invest Ophthalmol Vis Sci*. 2017;58:1499–1505.
 33. Dong J, Jia YD, Wu Q, et al. Interchangeability and reliability of macular perfusion parameter measurements using optical coherence tomography angiography. *Br J Ophthalmol*. 2017;101:1542–1549.
 34. Rabiolo A, Gelormini F, Marchese A, et al. Macular perfusion parameters in different angiocube sizes: does the size matter in quantitative optical coherence tomography angiography? *Invest Ophthalmol Vis Sci*. 2018;59:231–237.
 35. Chen FK, Menghini M, Hansen A, Mackey DA, Constable IJ, Sampson DM. Intrasession repeatability and interocular symmetry of foveal avascular zone and retinal vessel density in OCT angiography. *Transl Vis Sci Technol*. 2018;7:6.
 36. Gilat Schmidt T, Linderman RE, Strampe MR, Chui TYP, Rosen RB, Carroll J. The utility of frame averaging for automated algorithms in analyzing retinal vascular biomarkers in AngioVue OCTA. *Transl Vis Sci Technol*. 2019; 8:10.
 37. Mikhail M, Jiang S, Hahn P, Orlin A, Rao RC, Choudhry N. OCTA: a practical method of image averaging using adobe photoshop software. *Ophthalmic Surg Lasers Imaging*. 2019;50:802–807.
 38. Kaizu Y, Nakao S, Wada I, et al. Microaneurysm imaging using multiple en face OCT angiography image averaging: morphology and visualization. *Ophthalmol Retina*. 2020;4:175–186.
 39. Laueremann JL, Xu Y, Heiduschka P, et al. Impact of integrated multiple image averaging on OCT angiography image quality and quantitative parameters. *Graefes Arch Clin Exp Ophthalmol*. 2019;257:2623–2629.
 40. Yannuzzi LA, Rohrer KT, Tindel LJ, et al. Fluorescein angiography complication survey. *Ophthalmology*. 1986;93:611–617.
 41. Thévenaz P, Ruttimann UE, Unser M. A pyramid approach to subpixel registration based on intensity. *IEEE Trans Image Process*. 1998;7:27–41.
 42. Schneider CA, Rasband WS, Eliceiri KW. NIH Image to ImageJ: 25 years of image analysis. *Nat Methods*. 2012;9:671–675.
 43. Linderman RE, Cava JA, Salmon AE, et al. Visual acuity and foveal structure in eyes with fragmented foveal avascular zones. *Ophthalmol Retina*. 2019;4:535–544.
 44. Linderman R, Salmon AE, Strampe M, Russillo M, Khan J, Carroll J. Assessing the accuracy of foveal avascular zone measurements using optical coherence tomography angiography: segmentation and scaling. *Transl Vis Sci Technol*. 2017;6:16.
 45. Wilk MA, Dubis AM, Cooper RF, Summerfelt P, Dubra A, Carroll J. Assessing the spatial relationship between fixation and foveal specializations. *Vision Res*. 2017;132:53–61.
 46. Krawitz BD, Phillips E, Bavier RD, et al. Parafoveal nonperfusion analysis in diabetic retinopathy using optical coherence tomography angiography. *Transl Vis Sci Technol*. 2018;7:4.
 47. Arganda-Carreras I, Fernandez-Gonzales R, Munoz-Barruitia A, Ortiz-de-Solorzano C. 3D reconstruction of histological sections: application to mammary gland tissue. *Microsc Res Tech*. 2010;73:1019–1029.
 48. Schindelin J, Arganda-Carreras I, Frise E, et al. Fiji: an open-source platform for biological-image analysis. *Nat Methods*. 2012;9:676–682.
 49. Bland JM, Altman DG. Statistics notes: measurement error. *Br Med J (Clin Res Ed)*. 1996;313:744.
 50. Krawitz BD, Mo S, Geyman LS, et al. Acircularity index and axis ratio of the foveal avascular zone in diabetic eyes and healthy controls measured by optical coherence tomography angiography. *Vision Res*. 2017;139:177–186.
 51. Sampson DM, Gong P, An D, et al. Axial length variation impacts on superficial retinal vessel

- density and foveal avascular zone area measurements using optical coherence tomography angiography. *Invest Ophthalmol Vis Sci.* 2017;58:3065–3072.
52. Shihara H, Sakamoto T, Yamashita T, et al. Reproducibility and differences in area of foveal avascular zone measured by three different optical coherence tomographic angiography instruments. *Sci Rep.* 2017;7:9853.
53. De Carlo TE, Salz DA, Waheed NK, Bauman CR, Duker JS, Witkin AJ. Visualization of the retinal vasculature using wide-field montage optical coherence tomography angiography. *Ophthalmic Surg Lasers Imaging Retina.* 2015;46:611–616.